2-step QRM-MLBD using Detection Ordering for Single-Carrier Transmission

Katsuhiro TEMMA[†] Tetsuya YAMAMOTO[†] and Fumiyuki ADACHI[‡]

Dept. of Electrical and Communication Engineering, Graduate School of Engineering, Tohoku University
6-6-05 Aza-Aoba, Aramaki, Aoba-ku, Sendai, 980-8579 Japan

†{tenma, yamamoto}@mobile.ecei.tohoku.ac.jp, ‡adachi@ecei.tohoku.ac.jp

Abstract—**2-step maximum likelihood block signal detection employing QR decomposition and M-algorithm (QRM-MLBD) can significantly improve the bit error rate (BER) performance of single-carrier (SC) transmission while reducing the computational complexity compared to maximum likelihood detection (MLD). In 2-step QRM-MLBD, unreliable symbol candidates are removed by performing minimum mean square error based frequency-domain equalization (MMSE-FDE) prior to QRM-MLBD. However, a large number M of surviving paths is still required in the M-algorithm to achieve a BER performance close to the matched filter (MF) bound. In this paper, to remedy this problem, we introduce a detection ordering to 2-step QRM-MLBD. We will show by computer simulation that the use of detection ordering can achieve the same BER performance as 2-step QRM-MLBD while reducing the computational complexity.**

Keywords-component; Single-carrier, near maximum likelihood detection, MMSE-FDE, QR decomposition, M-algorithm

I. INTRODUCTION

The broadband wireless channel is composed of many propagation paths with different time delays and therefore, the channel becomes severely frequency-selective [1]. The minimum mean square error based frequency-domain equalization (MMSE-FDE) can improve the bit error rate (BER) performance of single-carrier (SC) transmission with a low computational complexity [2, 3]. However, a big performance gap from the matched filter (MF) bound [4] still exists due to the presence of the residual inter-symbol interference (ISI) after FDE [5]. Although the maximum likelihood detection (MLD) [6] is the optimum signal detection, its computational complexity is extremely high.

Maximum likelihood block signal detection employing QR decomposition and M-algorithm (QRM-MLBD) [7] was proposed for SC transmission over a frequency-selective fading channel [8, 9]. QRM-MLBD can achieve a BER performance close to the MF bound with less complexity than MLD. However, its computational complexity is still high. In order to reduce the computational complexity, we proposed 2-step QRM-MLBD [10, 11] which discards unreliable symbol candidates by performing MMSE-FDE prior to QRM-MLBD. However, a large number M of surviving paths is required in the M-algorithm to achieve a BER performance close to the MF bound. In this paper, to remedy this problem, we introduce the detection ordering. The idea of detection ordering was proposed for multiple-input multiple-output (MIMO) system based on the observation that channels have different conditions [12, 13]. However, in SC block transmission, the channel quality is the same for all symbols in the received signal block. Therefore, the detection ordering based on the received signal power cannot be applied.

In this paper, we introduce a detection ordering to 2-step QRM-MLBD for SC block transmission to reduce the required number M of surviving paths in M-algorithm. The detection ordering is performed based on the result of MMSE-FDE (the first step of 2-step QRM-MLBD). After discarding unreliable symbol candidates, detection order are sorted in the ascending order of the number of symbol candidates to be involved in the path metric computation in each stage of the M-algorithm. Therefore, the probability of removing the correct path at early stages can be reduced in the M-algorithm and hence, the value of M can be reduced.

The remainder of this paper is organized as follows. Sect. II shows the SC transmission with conventional QRM-MLBD. Sect. III presents 2-step QRM-MLBD using the detection ordering. In Sect. IV, we evaluate by computer simulation the BER performance achievable by 2-step QRM-MLBD using the detection ordering and discuss about the computational complexity. Sect. V offers the conclusion.

II. SC TRANSMISSION MODEL

A. Signal Representation

The SC transmission model is illustrated in Fig. 1. Throughout the paper, the T_s symbol-spaced discrete time representation is used. We assume a frequency-selective fading channel composed of symbol-spaced L distinct propagation paths. The received signal is a cyclic convolution of the transmitted signal block and the channel impulse response as long as the cyclic prefix (CP) is longer than the maximum channel time delay.

A block of N_c symbols is assumed to be transmitted. In this paper, the data symbol block is expressed using the vector form as $\mathbf{d}=[d(0),\ldots,d(N_c-1)]^T$ ($[.]^T$ denotes the transpose operation). The last N_g symbols of each block are copied as a CP and inserted into the guard interval (GI) placed at the beginning of each block.

At the receiver, N_c-point discrete Fourier transform (DFT) is applied to transform the received signal into the frequency-
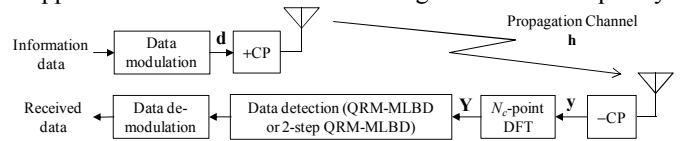

Figure 1.   SC transmission model.

domain signal. The frequency-domain received signal $\mathbf{Y}=[Y(0),\ldots,Y(N_c-1)]^T$ can be represented as

$$\mathbf{Y} = \sqrt{\frac{2E_s}{T_s}}\mathbf{HFd} + \mathbf{N} , \qquad (1)$$

where E_s is the symbol energy. $\mathbf{H}=diag[H(0),\ldots,H(N_c-1)]$ represents the frequency-domain channel gain matrix and $H(k) = \sum_{l=0}^{L-1} h_l \exp(-j2\pi k\tau_l / N_c)$, where h_l and τ_l are the complex-valued path gain with $E[\sum_{l=0}^{L-1}|h_l|^2]=1$ and the time delay of the lth path, respectively. The time delay of each propagation path is assumed to be an integer multiple of the symbol duration. $\mathbf{N}=[N(0),\ldots,N(N_c-1)]^T$ is the frequency-domain noise vector whose elements are independent zero-mean additive white Gaussian variables having the variance $2N_0/T_s$, N_0 is the one-sided power spectrum density of the additive white Gaussian noise. $\mathbf{F}$ is the DFT matrix given by

$$\mathbf{F} = \frac{1}{\sqrt{N_c}}\begin{bmatrix} 1 & 1 & \cdots & 1 \\ 1 & e^{-j2\pi\frac{1\times 1}{N_c}} & \cdots & e^{-j2\pi\frac{1\times(N_c-1)}{N_c}} \\ \vdots & \vdots & \ddots & \vdots \\ 1 & e^{-j2\pi\frac{(N_c-1)\times 1}{N_c}} & \cdots & e^{-j2\pi\frac{(N_c-1)\times(N_c-1)}{N_c}} \end{bmatrix}. \qquad (2)$$

B. Conventional QRM-MLBD

A concatenation of propagation channel $\mathbf{H}$ and DFT matrix $\mathbf{F}$ can be viewed as an equivalent channel $\overline{\mathbf{H}} = \mathbf{HF}$. By applying the QR decomposition to the equivalent channel matrix as $\overline{\mathbf{H}} = \mathbf{QR}$, where $\mathbf{Q}$ is an $N_c \times N_c$ unitary matrix and $\mathbf{R}$ is an $N_c \times N_c$ upper triangular matrix and then multiplying $\mathbf{Y}$ by $\mathbf{Q}^H$, the transformed received signal $\mathbf{Z}=[Z(0),\ldots,Z(N_c-1)]^T$ is obtained as

$$\begin{aligned} \mathbf{Z} &= \mathbf{Q}^H\mathbf{Y} = \sqrt{\frac{2E_s}{T_s}}\mathbf{Rd} + \mathbf{Q}^H\mathbf{N} \\ &= \sqrt{\frac{2E_s}{T_s}}\begin{bmatrix} R_{0,0} & \cdots & R_{0,N_c-1} \\ & \ddots & \vdots \\ \mathbf{0} & & R_{N_c-1,N_c-1} \end{bmatrix}\begin{bmatrix} d(0) \\ \vdots \\ d(N_c-1) \end{bmatrix} + \mathbf{Q}^H\mathbf{N} \end{aligned} \qquad (3)$$

From Eq. (3), the ML decision on the transmitted block can be efficiently performed by searching for the best path having the minimum squared Euclidean distance in the tree diagram composed of N_c stages. A full tree-search is required to achieve the ML solution, however, this results in very high computational complexity. In order to reduce the computational complexity in the tree-search, the M-algorithm [14] is used in QRM-MLBD.

III. 2-STEP QRM-MLBD WITH DETECTION ORDERING

In the first step of 2-step QRM-MLBD, the symbol candidates to be involved in the path metric computation are selected by performing MMSE-FDE prior to QRM-MLBD in order to prune some of the symbol candidates in the tree. The selection of symbol candidates is done based on the Euclidean distance between either hard decision [10] or soft decision

results of MMSE-FDE [11] and symbol candidates. In this paper, we call the former as "2-step hard QRM-MLBD" and the latter as "2-step soft QRM-MLBD".

In the first step of 2-step QRM-MLBD, MMSE-FDE is carried out by multiplying $\mathbf{Y}$ by the MMSE weight matrix $\mathbf{W}$ as [2, 3]

$$\widetilde{\mathbf{D}} = \mathbf{WY} , \qquad (4)$$

where

$$\mathbf{Y} = \sqrt{\frac{2E_s}{T_s}}\mathbf{HD} + \mathbf{N} , \qquad (5)$$

$$\mathbf{W} = diag\left[\frac{H^*(0)}{|H(0)|^2 + N_0/E_s}, \cdots, \frac{H^*(N_c-1)}{|H(N_c-1)|^2 + N_0/E_s} \right], \quad (6)$$

$\mathbf{D}=\mathbf{Fd}=[D(0),\ldots,D(N_c-1)]$ is the frequency-domain transmitted signal vector, and $[.]^*$ denotes the complex conjugate operation. By applying N_c-point inverse DFT (IDFT) to $\widetilde{\mathbf{D}} = [\widetilde{D}(0),\ldots,\widetilde{D}(N_c-1)]^T$, the soft decision symbol vector $\widetilde{\mathbf{d}} = [\widetilde{d}(0),\ldots,\widetilde{d}(N_c-1)]^T$ is obtained as

$$\widetilde{\mathbf{d}} = \mathbf{F}^H\widetilde{\mathbf{D}} , \qquad (7)$$

based on which unreliable symbol candidates to be discarded are determined.

A. 2-step hard QRM-MLBD [10]

The symbol candidates within the distance R from the MMSE-FDE hard detection results are selected and others are discarded. Figure 2 shows how to select the reliable symbol candidates for 16QAM case, where $R = 2/\sqrt{5}$ is used [10].

The number $N_{cand}^{(i)}$ of the symbol candidates to be involved in the path metric computation at the ith stage, $i=0\sim N_c-1$, takes a value from $\{4,6,9\}$ and the average is given by $(1/N_c)\sum_{i=0}^{N_c-1} N_{cand}^{(i)} = 6.25$.

B. 2-step soft QRM-MLBD [11]

The soft decision symbol $\widetilde{d}(t)$ can be expressed as

$$\widetilde{d}(t) = \sqrt{\frac{2E_s}{T_s}}\left(\frac{1}{N_c}\sum_{k=0}^{N_c-1}\widetilde{H}(k) \right)d(t) + \mu_{ISI}(t) + \mu_{noise}(t) , \quad (8)$$

where $\widetilde{H}(k)=W(k)H(k)$ is the frequency-domain channel gain at the kth frequency after MMSE-FDE. In Eq. (8), the first, second, and third terms are the desired signal, residual ISI, and
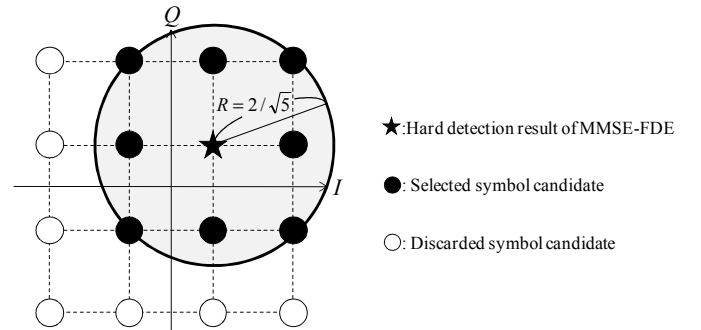

Figure 2.   Symbol candidate selection in 2-step hard QRM-MLBD.

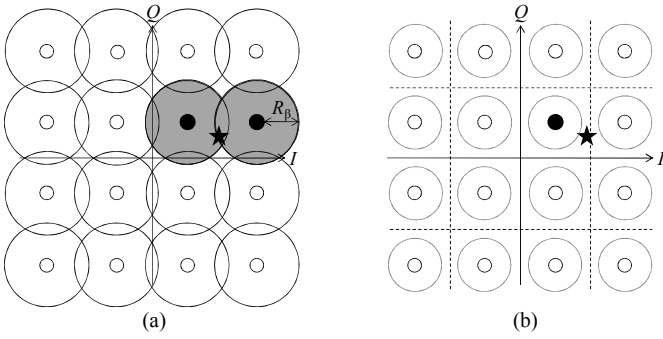(a)   (b)

Figure 3.   Symbol candidate selection in 2-step soft QRM-MLBD.
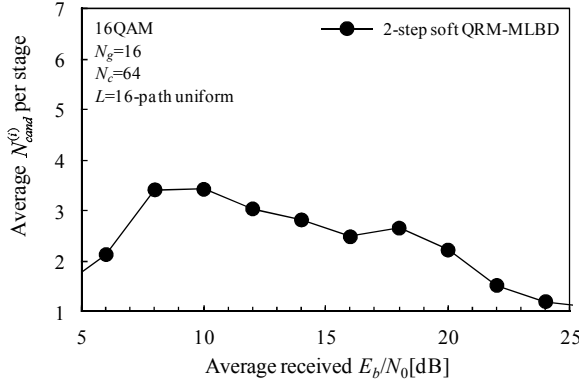

Figure 4.   Average $N_{cand}^{(i)}$ per stage for 2-step soft QRM-MLBD.

noise components, respectively. $\widetilde{d}(t)$ is normalized by $A = \sqrt{2E_s/T_s}\{(1/N_c)\sum_{k=0}^{N_c-1}\widetilde{H}(k)\}$ to obtain

$$\widetilde{d}'(t) = d(t) + \mu'_{ISI}(t) + \mu'_{noise}(t),\qquad (9)$$

where

$$\mu'_{ISI}(t) = \frac{A^{-1}}{N_c}\sqrt{\frac{2E_s}{T_s}}\sum_{k=0}^{N_c-1}\widetilde{H}(k)\sum_{n=0\neq t}^{N_c-1} d(n)\exp\left(j2\pi k\frac{t-n}{N_c}\right)\quad (10)$$

$$\mu'_{noise}(t) = \frac{A^{-1}}{N_c}\sum_{k=0}^{N_c-1}\widetilde{N}(k)\exp\left(j2\pi k\frac{t}{N_c}\right)\qquad (11)$$

with $\widetilde{N}(k) = W(k)N(k)$ representing the noise component after MMSE-FDE. The residual ISI plus noise component $\mu(t) = \mu'_{ISI}(t) + \mu'_{noise}(t)$ can be treated as a new zero-mean complex Gaussian variable [4] and the variance σ_μ^2 of $\mu(t)$ is given by

$$\sigma_\mu^2 = \frac{1}{2}E[|\mu(t)|^2] = \sigma_{ISI}^2 + \sigma_{noise}^2 \qquad (12)$$

$$\sigma_{ISI}^2 = A^{-2}\frac{E_s}{T_s}\left[\frac{1}{N_c}\sum_{k=0}^{N_c-1}\left|\widetilde{H}(k)\right|^2 - \left|\frac{1}{N_c}\sum_{k=0}^{N_c-1}\widetilde{H}(k)\right|^2\right] \qquad (13)$$

$$\sigma_{noise}^2 = A^{-2}\frac{1}{N_c}\frac{N_0}{T_s}\sum_{k=0}^{N_c-1}\left|W(k)\right|^2. \qquad (14)$$

In the 2-step soft QRM-MLBD, the symbol candidates are selected by drawing the circle centered at each symbol candidate in the signal constellation. The radius R_β of the circle, outside which r falls with the probability β, is given as [10]

$$R_\beta = \sqrt{-2\sigma_\mu^2 \ln\beta}. \qquad (15)$$

The symbol candidates whose distance from the normalized soft decision output of MMSE-FDE is shorter than R_β are selected as reliable ones and others are discarded as unreliable ones, as shown in Fig. 3(a). When no symbol is selected, only the hard decision result of MMSE-FDE is selected as in Fig. 3(b).

If small β is used, better BER performance can be achieved, but the computational complexity is high. As β is increased, the computational complexity decreases, but this results in BER degradation. Considering this tradeoff between computational complexity and BER performance, we found, by the preliminary computer simulation, the optimal value of β at each average received E_b/N_0 for the given channel power delay profile and data modulation.

The number $N_{cand}^{(i)}$, $i=0\sim N_c-1$, of the symbol candidates to be involved in the path metric computation at the ith stage takes a value between 1 and X. The average $N_{cand}^{(i)}$ is plotted in Fig. 4.

C. Introduction of Detection Ordering

When M is small, the probability of removing the correct path at early stages in the M-algorithm is high because the elements of **R** closer to right positions tend to drop with a larger probability [15] and hence, the reliability of path metric in early stages is low [16, 17]. Therefore, the value of M cannot be too small. In this paper, in order to reduce the required number M of surviving paths, we introduce the detection ordering based on the result of symbol candidate selection into the first step.

Figure 5(a) shows an example of tree diagram for conventional QRM-MLBD, as described in Sect. II-B. Note that for conventional QRM-MLBD, $N_{cand}^{(i)} = X$, $i=0\sim N_c-1$. In 2-step QRM-MLBD, the symbol candidates to be involved in the path metric computation are selected in the first step. The detection order is determined by sorting the symbols $d(0)\sim d(N_c-1)$ in ascending order of $\{N_{cand}^{(i)}; 0 \sim N_c-1\}$. An example is shown in Fig. 5(b) assuming a three-symbol block with the 2-step soft QRM-MLBD. The frequency-domain received signal is given as

$$\begin{bmatrix} Y(0) \\ Y(1) \\ Y(2) \end{bmatrix} = \sqrt{\frac{2E_s}{T_s}}\begin{bmatrix} \overline{H}_{0,0} & \overline{H}_{0,1} & \overline{H}_{0,2} \\ \overline{H}_{1,0} & \overline{H}_{1,1} & \overline{H}_{1,2} \\ \overline{H}_{2,0} & \overline{H}_{2,1} & \overline{H}_{2,2} \end{bmatrix}\begin{bmatrix} d(0\,|\,N_{cand}^{(0)}=2) \\ d(1\,|\,N_{cand}^{(1)}=1) \\ d(2\,|\,N_{cand}^{(2)}=3) \end{bmatrix} + \mathbf{N}, \qquad (16)$$

where $d(i\,|\,N_{cand}^{(i)}=j)$ denotes the ith symbol whose corresponding stage has j symbol candidates. The received signal after the detection ordering can be written as

$$\begin{bmatrix} Y(0) \\ Y(1) \\ Y(2) \end{bmatrix} = \sqrt{\frac{2E_s}{T_s}}\begin{bmatrix} \overline{H}_{0,2} & \overline{H}_{0,0} & \overline{H}_{0,1} \\ \overline{H}_{1,2} & \overline{H}_{1,0} & \overline{H}_{1,1} \\ \overline{H}_{2,2} & \overline{H}_{2,0} & \overline{H}_{2,1} \end{bmatrix}\begin{bmatrix} d(2\,|\,N_{cand}^{(2)}=3) \\ d(0\,|\,N_{cand}^{(0)}=2) \\ d(1\,|\,N_{cand}^{(1)}=1) \end{bmatrix} + \mathbf{N}. \qquad (17)$$

(a) Conventional QRM-MLBD

(b) 2-step soft QRM-MLBD
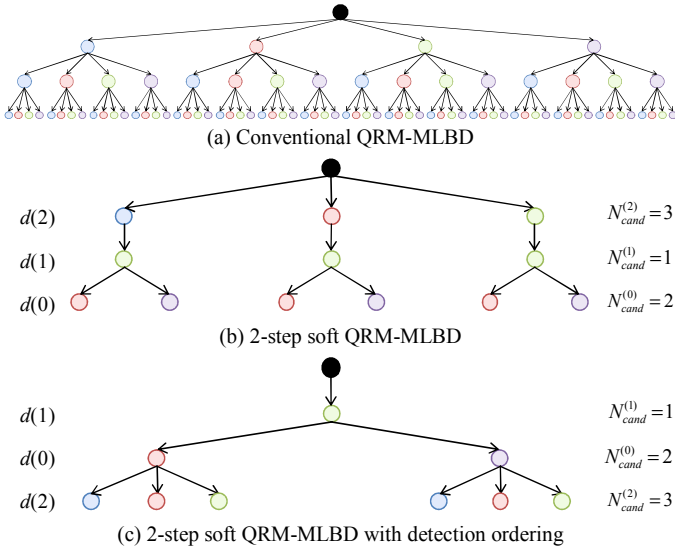
(c) 2-step soft QRM-MLBD with detection ordering

Figure 5.   An example of tree structure comparison (QPSK and N_c=3).

After the detection ordering, the tree structure is reconstructed as shown in Fig. 5(c). Using the detection ordering, the number of paths in early stages can be reduced and therefore, the probability of removing the correct path in the M-algorithm can be reduced even if a small M is used.

IV.   COMPUTER SIMULATION

We evaluate the average BER performance and computational complexity by computer simulation. We assume 16QAM data modulation, block size N_c=64, and GI size N_g=16. The channel is assumed to be a frequency-selective block Rayleigh fading channel having symbol-spaced L=16-path uniform power delay profile. Ideal channel estimation is assumed.

Figure 6 shows the average BER performance comparison between 2-step QRM-MLBD with and without detection ordering. For comparison, the BER performance of conventional QRM-MLBD with M=256 is also shown. When M is small, the probability of removing the correct path at early stages may increase and therefore, the use of detection ordering is particularly effective for small M cases. It can be seen from Fig. 6 that M=64 is sufficient for achieving a close-to-MF bound performance for 2-step soft QRM-MLBD while M=256 is needed for 2-step hard QRM-MLBD. This is because 2-step soft QRM-MLBD can reduce the number of symbol candidates to be involved in the path metric computation more than 2-step hard QRM-MLBD and therefore, the introduction of ordering can further reduce the number of candidate in an early stage of 2-step soft QRM-MLBD compared to 2-step hard QRM-MLBD.

The computational complexity comparison between conventional QRM-MLBD and 2-step QRM-MLBDs is done in terms of the number of complex multiplications per block of N_c symbols. Table I shows the number of complex multiplications per block of N_c symbols. 2-step hard and soft QRM-MLBD involves MMSE-FDE prior to QRM-MLBD. 2-step soft QRM-MLBD requires the computation of variance

σ_μ^2 of residual ISI plus noise after MMSE-FDE and the symbol candidate selection (i.e. computation of the distances between soft decision output of MMSE-FDE and symbol candidates). 2-step hard and soft QRM-MLBD significantly reduces the path metric computation and hence reduces the total computational complexity compared to QRM-MLBD. Furthermore, the use of detection ordering can further reduce the path metric computation. However, to achieve a close to MF bound performance, M=256 is still required for the case of 2-step hard QRM-MLBD. However, M=64 is sufficient for the case of 2-step soft QRM-MLBD.
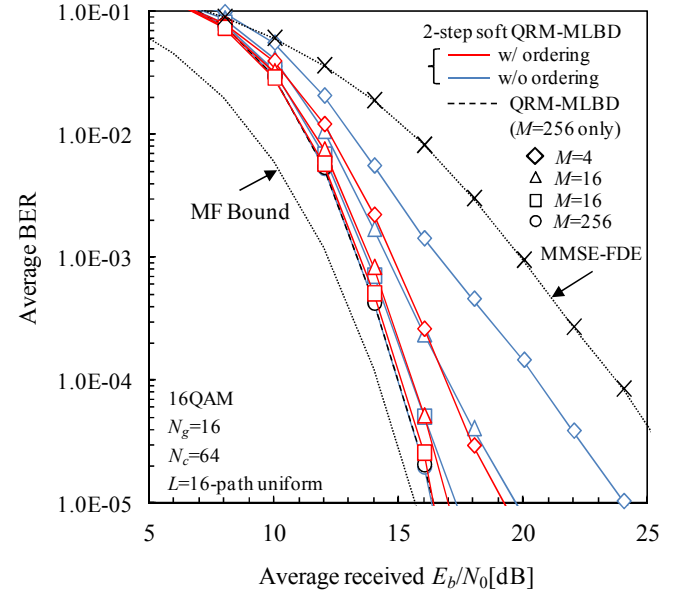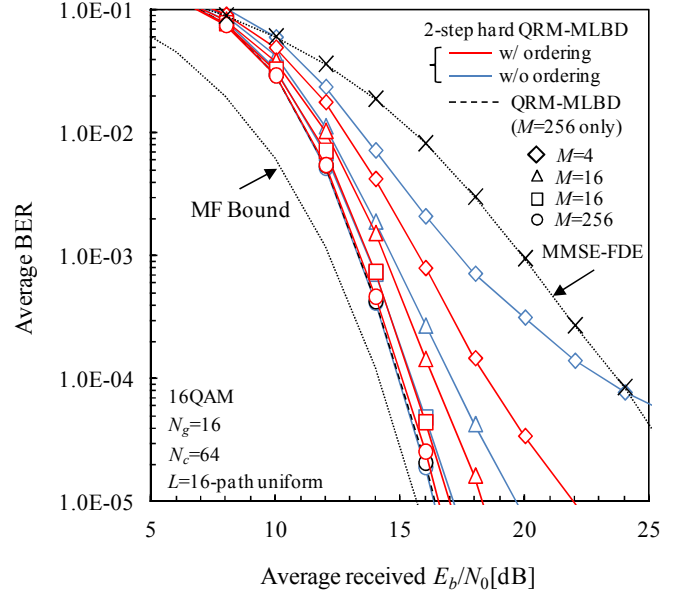

(a) 2-step hard QRM-MLBD with and without ordering

(b) 2-step soft QRM-MLBD with and without ordering

Figure 6.   BER performance comparison.

REFERENCES

[1] J. G. Proakis and M. Salehi, *Digital communications*, 5th ed., McGraw-Hill, 2008.

[2] D. Falconer, S. L. Ariyavisitakul, A. Benyamin- Seeyar, and B. Edison, "Frequency domain equalization for single-carrier broadband wireless systems," IEEE Commun. Mag., Vol. 40, No. 4, pp. 58-66, Apr. 2002..

[3] F. Adachi, T. Sao, and T. Itagaki, "Performance of multicode DS-CDMA using frequency domain equalization in a frequency selective fading channel," IEE Electronics Letters, Vol. 39, No.2, pp. 239-241, Jan. 2003.

[4] F. Adachi and K. Takeda, "Bit error rate analysis of DS-CDMA with joint frequency-domain equalization and antenna diversity combining," IEICE Trans. Commun., Vol. E87-B, No. 10, pp.2991-3002, Oct. 2004.

[5] K. Takeda, K. Ishihara, and F. Adachi, "Frequency-domain ICI cancellation with MMSE equalization for DS-CDMA downlink," IEICE Trans. Commun., Vol. E89-B, No. 12, pp. 3335-3343, Dec. 2006.

[6] A. van Zelst, R. van Nee, and G. A. Awater, "Space division multiplexing (SDM) for OFDM systems," Proc. IEEE 51st Vehicular Technology Conference (VTC), pp. 1070-1074, May 2000.

[7] L. J. Kim and J. Yue, "Joint channel estimation and data detection algorithms for MIMO-OFDM systems," Proc. Thirty-Sixth Asilomar Conference on Signals, System and Computers, pp. 1857-1861, Nov. 2002.

[8] K. Nagatomi, K. Higuchi, and H. Kawai "Complexity reduced MLD based on QR decomposition in OFDM MIMO multiplexing with frequency domain spreading and code multiplexing," Proc. IEEE Wireless Communications and Networking Conference (WCNC 2009), pp. 1-6, Apr. 2009.

[9] T. Yamamoto, K. Takeda, and F. Adachi, "Single-carrier transmission using QRM-MLD with antenna diversity," Proc. The 12th International Symposium on Wireless Personal Multimedia Communications (WPMC 2009), Sendai, Japan, Sept. 2009.

[10] K. Temma, T. Yamamoto, and F. Adachi, "Computationally efficient 2-step QRM-MLD for single-carrier transmissions," Proc. The IEEE International Conference on Communication Systems (IEEE ICCS 2010), Singapore, 17-19, Nov. 2010.

[11] K. Temma, T. Yamamoto, and F. Adachi, "Improved Decision 2-step QRM-ML Block Signal Detection for Single-Carrier Transmission," 2011 IEEE 74th Vehicular Technology Conference (VTC2011-Fall), San Francisco, United States, 5-8 Sep. 2011.

[12] D. Wübben, R. Böhnke, J. Rinas, V. Kühn, and K. D. Kammeyer, "Efficient algorithm for decoding layered space-time codes," IEE Electronics Letters, vol. 37, no. 22, pp. 1348-1350, October 2001.

[13] K. J. Kim, J. Yue, R. A. Iltis and J. D. Glibson, "A QRD-M/Kalman filter-based detection and channel estimation algorithm for MIMO-OFDM systems," *IEEE Trans. Wireless Commun.*, vol. 4, no. 2, pp. 710–421, Mar. 2005.

[14] J. B. Anderson and S. Mohan, "Sequential coding algorithms: A survey and cost analysis," IEEE Trans. on Commun., Vol. 32, pp. 169-176, Feb. 1984.

[15] K. Takeda, H. Tomeba, and F. Adachi, "Joint Tomlinson-Harashima precoding and frequency-domain equalization for broadband single-carrier transmission," IEICE Trans. Commun., Vol. E91-B, No. 1, pp. 258-266, 2008.

[16] T. Yamamoto, K. Takeda, and F. Adachi, "Training sequence aided single-carrier block signal detection using QRM-MLD," Proc. IEEE Wireless Communication & Networking Conference (WCNC), Apr. 2010.

[17] T. Yamamoto, K. Takeda, and F. Adachi, "MMSE based QRM-MLD Frequency-domain block signal detection for single-carrier transmission," Proc. The 7th IEEE VTS Asia Pacific Wireless Communication Symposium (APWCS 2010), Taiwan, May 2010

TABLE I.   THE NUMBER OF COMPLEX MULTIPLICATIONS

	QRM-MLBD	2-step QRM-MLBD	
		hard	soft
Fast Fourier transform (FFT)	$N_c\log_2 N_c$		
MMSE-weight computation & FDE		$2N_c$	
Inverse FFT (IFFT)	$N_c\log_2 N_c$		
Computation of **HF**	N_c^2		
Computation of σ_μ^2			$3N_c+1$
Symbol candidate selection			XN_c
QR decomposition	N_c^3		
Computation of $\mathbf{Q}^H\mathbf{Y}$	N_c^2		
Path metric computation	$X\{2+(M/2)(N_c+4)(N_c-1)\}$	$E[N_{cand}^{(i)}]\{2+(M/2)(N_c+4)(N_c-1)\}$	

TABLE II.   EXAMPLE OF THE NUMBER OF COMPLEX MULTIPLICATIONS

	QRM-MLBD	2-step soft QRM-MLBD	
		w/o ordering	w/ordering
Fast Fourier transform (FFT)	384		
MMSE-weight computation & FDE		128	
Inverse FFT (IFFT)	384		
Computation of **HF**	4096		
Computation of σ_μ^2		193	
Symbol candidate selection		1024	
QR decomposition	262114		
Computation of $\mathbf{Q}^H\mathbf{Y}$	4096		
Path metric computation	8773664 (X=16, M=256)	1544495 ($E[N_{cand}^{(i)}]$=2.82, M=256)	386128 ($E[N_{cand}^{(i)}]$=2.82, M=64)
Total	9044384	1816914	658577

Table II shows the number of complex multiplications per block of N_c=64 symbols required for achieving average BER=10^{-3} (average received E_b/N_0=14dB). The 2-step soft QRM-MLBD with detection ordering requires only 7.3% (36%) of the average complexity of the conventional QRM-MLBD (2-step soft QRM-MLBD without detection ordering) when 16QAM data modulation is used.

V.   CONCLUSIONS

In this paper, we proposed the detection ordering based on the result of symbol candidate selection for 2-step QRM-MLBD in order to reduce the number M of surviving paths in M-algorithm. The proposed ordering aims to reduce the number of paths and the probability of removing correct path in early stages of the M-algorithm. We discussed the effect of detection ordering. We showed that 2-step soft QRM-MLBD with detection ordering can reduce the required value of M from 256 to 64 for achieving close to MF bound performance. 2-step soft QRM-MLBD with detection ordering requires only 7.3% (36%) of the average complexity of the conventional QRM-MLBD (2-step soft QRM-MLBD without detection ordering) when 16QAM data modulation is used.